SCIENTIFIC REPORTS
nature research

OPEN

A role of the Nse4 kleisin and Nse1/Nse3 KITE subunits in the ATPase cycle of SMC5/6

Lucie Vondrova[1], Peter Kolesar[1], Marek Adamus[2], Matej Nociar[1], Antony W. Oliver[3] & Jan J. Palecek[1,2] ✉

The SMC (Structural Maintenance of Chromosomes) complexes are composed of SMC dimers, kleisin and kleisin-interacting (HAWK or KITE) subunits. Mutual interactions of these subunits constitute the basal architecture of the SMC complexes. In addition, binding of ATP molecules to the SMC subunits and their hydrolysis drive dynamics of these complexes. Here, we developed new systems to follow the interactions between SMC5/6 subunits and the relative stability of the complex. First, we show that the N-terminal domain of the Nse4 kleisin molecule binds to the SMC6 neck and bridges it to the SMC5 head. Second, binding of the Nse1 and Nse3 KITE proteins to the Nse4 linker increased stability of the ATP-free SMC5/6 complex. In contrast, binding of ATP to SMC5/6 containing KITE subunits significantly decreased its stability. Elongation of the Nse4 linker partially suppressed instability of the ATP-bound complex, suggesting that the binding of the KITE proteins to the Nse4 linker constrains its limited size. Our data suggest that the KITE proteins may shape the Nse4 linker to fit the ATP-free complex optimally and to facilitate opening of the complex upon ATP binding. This mechanism suggests an important role of the KITE subunits in the dynamics of the SMC5/6 complexes.

The SMC (Structural Maintenance of Chromosomes) complexes are key organizers of prokaryotic and eukaryotic genomes. They organize chromatin domains (cohesins[1]), condense mitotic chromosomes (condensins[2]), assist in DNA repair (SMC5/6[3,4]) and replication (SMC/ScpAB[5]). These circular complexes use the energy of ATP hydrolysis to drive DNA topology changes. In prokaryotes, SMC/ScpAB drives extrusion of loops behind the replication fork. In eukaryotes, condensins extrude loops laterally and axially to shape chromatin to the typical mitotic chromosomes. Cohesins assist in formation of topologically associating domains during interphase. Cohesin rings can also hold newly replicated sister chromatids together and release them in highly controlled manner. The SMC5/6 complexes have been implicated in the repair of DNA damage by homologous recombination, and in stabilization and restart of stressed replication forks. The SMC5/6 instability leads to the chromosome breakage syndrome in human[6], however, the molecular mechanism of the SMC5/6 action is largely unclear.

All the SMC complexes are composed of three common categories of subunits: SMC, kleisin and kleisin-interacting proteins[7,8]. The SMC proteins are primarily built of long anti-parallel coiled-coil arms, a globular hinge (situated in the middle of the peptide chain) and a head domain (formed by combined amino and carboxyl termini[9–13]). The globular head domain contains ATP binding and hydrolysis motifs of the ATP-binding cassette transporter family[14,15]. Two SMC molecules form dimers via the association of their hinge domains and transiently interact when their head domains sandwich a pair of ATP molecules. The binding of ATP changes conformation and shape of the SMC subunits at local as well as global levels[10]. At local level, the SMC heads and necks move from aligned position to the ATP-locked conformation. At global level, the overall shape of the complex changes from rod- to ring-like upon ATP binding (with heads locked by ATP at one end and hinge dimer at the other end). The hydrolysis of ATP dissolves the SMC-ATP-SMC head bridge.

The ATPase head domains are also connected by the kleisin subunit in an asymmetric way. Kleisin binds to the cap side of one SMC (designated as κSMC) head domain via a winged-helix domain (WHD) at its carboxyl terminus. Kleisin's α-helix located at its amino terminal helix-turn-helix (HTH) domain binds to the coiled-coil base region immediately adjacent to the other SMC head (called neck and designated as νSMC[16–18]). This kleisin

[1]National Centre for Biomolecular Research, Faculty of Science, Masaryk University, Kamenice 5, 62500, Brno, Czech Republic. [2]Mendel Centre for Plant Genomics and Proteomics, Central European Institute of Technology, Masaryk University, Kamenice 5, 62500, Brno, Czech Republic. [3]Genome Damage and Stability Centre, School of Life Sciences, University of Sussex, Falmer, Brighton, BN1 9RQ, United Kingdom. ✉e-mail: jpalecek@sci.muni.cz

bridge mediated by protein-protein interactions seems to be more permanent than the ATP-mediated bridge (as the latter bridge dissolves upon ATP hydrolysis). However, the ATP binding may induce dissociation of the kleisin-νSMC interaction and lead to release of DNA from the ring[19–25].

The kleisin-interacting subunits bind and shape kleisin linker regions connecting N- and C-terminal domains. The KITE (Kleisin-Interacting Tandem winged-helix Element) subunits interact with kleisins in prokaryotic SMC/ScpAB and eukaryotic SMC5/6 complexes, while eukaryotic cohesin and condensin complexes associate with HAWK (HEAT proteins Associated With Kleisin) proteins[7,8]. Interestingly, the HAWK (Scc3 and Pds5) and Wapl proteins regulate release of cohesin from chromosomes. It was proposed that these proteins shape and stiffen the linker region of the kleisin molecule, which assists in transduction of conformational changes of the ATP-mediated SMC head dimerization to the dissociation of the kleisin-νSMC interaction (Scc1-Smc3 in the cohesin complex[19–22,24]). Similarly, the KITE proteins assist in opening of the SMC/ScpAB complex[26,27]. However, the role of the KITE subunits in the SMC5/6 complex remains largely elusive.

Here, we aimed to uncover relationships between SMC5/6 subunits and their roles in the SMC5/6 dynamics. We developed new systems to analyse the interactions between SMC5/6 subunits and to follow the stability of the SMC5/6 complexes. Using systems composed of SMC6-Nse4-Nse3-Nse1 and SMC6-Nse4-SMC5, respectively, we showed that the N-terminal HTH domain of the Nse4 kleisin molecule binds to the SMC6 neck and bridges it with the SMC5 head. With a more complex SMC6-SMC5-Nse4-Nse3-Nse1 system, we observed increased stability of the ATP-free SMC5/6 core complex upon binding of the Nse1 and Nse3 KITE proteins to the Nse4 kleisin. While the ATP-free complex was highly stable, the binding of ATP to the SMC5/6 core complex containing KITE-bound kleisin significantly decreased its relative stability. Reduced Nse3 binding to the Nse4 linker or elongation of the Nse4 linker partially suppressed the instability of the ATP-bound complex, suggesting that the binding of the KITE proteins to the Nse4 linker constrains its limited size. Our data suggest that the KITE proteins may shape the Nse4 linker to fit the ATP-free complex optimally and to facilitate opening of the complex upon ATP binding.

Results

Nse4 interacts with SMC6 neck. We have previously shown that Nse4 belongs to the kleisin superfamily of proteins and binds to the SMC5 and SMC6 head fragments[28]. To map the Nse4 interaction with SMC6, we employed peptide library covering yeast *S. pombe* SMC6 region aa875-1024 (Supplementary Table 1). The peptides were pre-bound to ELISA plates and tested against Nse4(1-150) and control (human TRF2) proteins[29]. The peptides covering the C-terminal region of SMC6 (aa955-1009) bound to Nse4 (Suppl. Fig. S1A). The peptide aa960-984 exhibited the highest affinity and specificity to Nse4, while the other peptides bound to Nse4 in a less specific way (e.g. peptide aa970-994). Interestingly, the SMC6 region aa960-984 corresponds to the SMC neck regions interacting with kleisins in most SMC complexes[12] (Fig. 1A).

To analyse the Nse4-SMC6 interaction in more detail, we established various multicomponent yeast two-hybrid (mY2H) systems[30]. It was difficult to follow the Nse4-SMC6 binary interaction in classical Y2H (Fig. 1B, column 3[28,31,32]), therefore we added DNA encoding Nse1 and Nse3 subunits on an extra plasmid (p416ADH1-Nse1 + Nse3 construct; 4Y2H) to enhance the Nse4-binding properties[33]. Indeed, addition of both Nse1 and Nse3 subunits to Gal4BD-Nse4/Gal4AD-SMC6 resulted in a relatively stable SMC6-Nse4-Nse3-Nse1 complex (Fig. 1B, column 4). Similarly, addition of SMC5 to Nse4-SMC6 (3Y2H) resulted in formation of a relatively stable SMC5-Nse4-SMC6 complex (Fig. 1C, column 4).

Using these mY2H systems and site-directed mutagenesis, we aimed to identify the Nse4-binding residues within the most conserved part of the ELISA-defined SMC6 region (aa960-984; Figs. 1A and S1A). The L964A, L965A, L968A, E969A, L972A and R975A mutations reduced stability of the SMC6-Nse4-Nse3-Nse1 tetramer, while the others had negligible effect (Figs. 1B and S1B). These data suggest that residues L964, L965, L968, E969, L972 and R975 may mediate either the Nse4-SMC6 interaction or putative interactions between SMC6 and Nse1-Nse3 subunits. To exclude the latter possibility, we employed 3Y2H system consisting of the SMC5-SMC6-Nse4 subunits. Again, L964A, L965A, L968A, E969A, L972A and R975A mutations reduced stability of the (SMC5-)SMC6-Nse4 complex, while the others had no effect (Figs. 1C and S1C), suggesting that these residues may mediate the Nse4-SMC6 interaction or affect multiple SMC6 interactions.

To distinguish mutations specifically disturbing the Nse4-SMC6 interaction from those affecting the multiple SMC6 interactions (e.g. by protein structure and stability alteration), we established another 3Y2H system consisting of the SMC6 and Nse5-Nse6 subunits (as Nse5 and Nse6 bind to the SMC6 protein[28]). In this system, we used the same Gal4AD-SMC6 mutation constructs as above in combination with Gal4BD-Nse5 and p416ADH1-Nse6 (Figs. 1D and S1D). The L964A, L968A and E969A mutations reduced SMC6-Nse5-Nse6 complex stability, suggesting their deleterious effects on the SMC6 interactions in general (Fig. 1, compare panels B, C and D, columns 5, 7 and 8). Note that the protein levels of the SMC6/L968A and SMC6/E969A mutants were lower compared to the wild-type Gal4AD-SMC6, suggesting their destabilizing effect (Suppl. Fig. S1E, lanes 7 and 8). In contrast, the other mutations had no impact on the SMC6-Nse5-Nse6 stability, suggesting that the conserved L965, L972 and R975 residues within the SMC6 neck region mediate specifically the SMC6-Nse4 interaction (Figs. 1 and S1).

SMC6 binds the N-terminal motif of the Nse4 protein. Next, we took advantage of the crystal structures of the kleisin-νSMC complexes[16–18,25,27], which suggested a key role for the N-terminal HTH domain of the kleisin molecule in its binding to νSMC neck. We mutated residues within the third α-helix of the Nse4 HTH domain (aa62-68) and analysed their impact on the Nse4-SMC6 interaction using the SMC6-Nse4-Nse3-Nse1 4Y2H and SMC5-Nse4-SMC6 3Y2H systems as above (Fig. 1B,C). The Nse4 mutations L62C, K64C, T65R, D67C and L68C reduced the stability of the Nse4-SMC6 complexes significantly, while the others had no effect (Fig. 2A,B). To distinguish between mutations specifically disturbing Nse4-SMC6 interactions and mutations

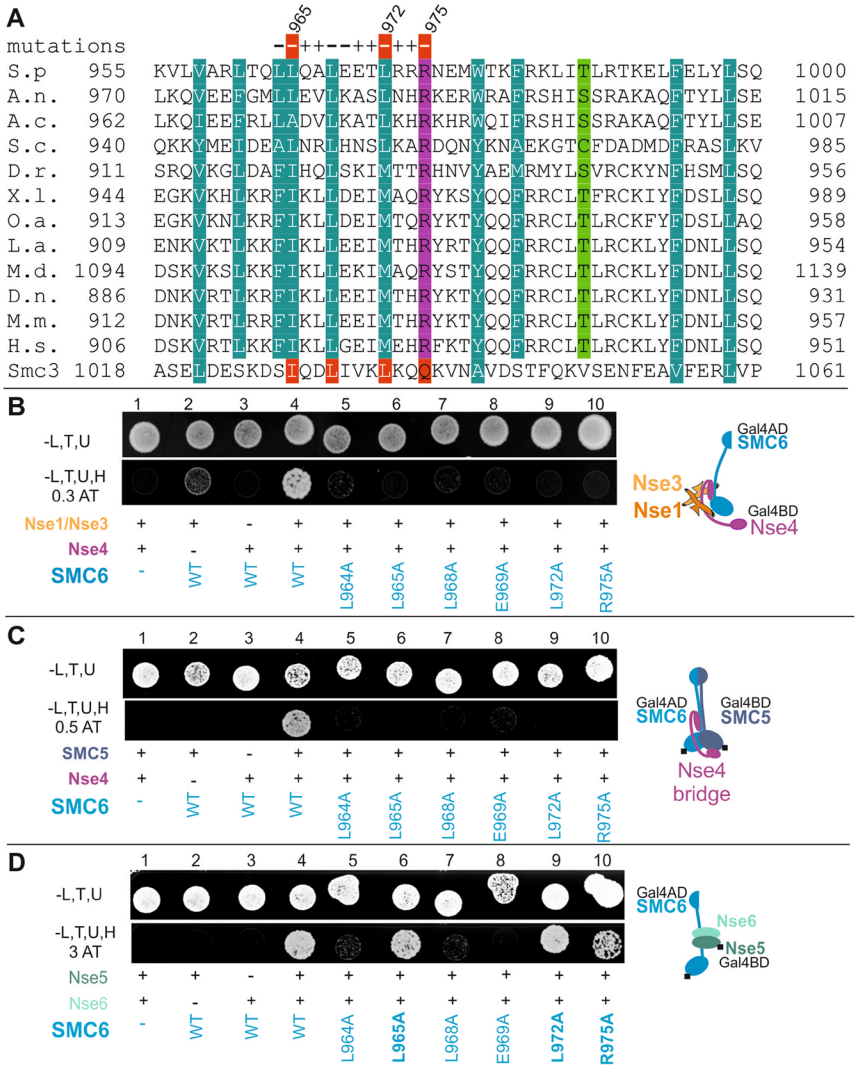

Figure 1. Nse4 binds neck region of the SMC6 protein. (**A**) Alignment of the C-terminal SMC6 neck region. The SMC6 orthologs are from *Schizosaccharomyces pombe* (*S.p.*), *Aspergillus nidulans* (*A.n.*), *Aspergillus clavatus* (*A.c.*), *S. cerevisiae* (*S.c.*), *Danio rerio* (*D.r.*), *Xenopus laevis* (*X.l.*), *Ornithorhynchus anatinus* (*O.a.*), *Loxodonta africana* (*L.a.*), *Monodelphis domestica* (*M.d.*), *Dasypus novemcinctus* (*D.n.*), *Mus musculus* (*M.m.*), *Homo sapiens* (*H.s.*). The SMC3 sequence from *S. cerevisiae* represents SMC binding mode present in the SMC3-Scc1 crystal structure (PDB: 4UX3). "+", mutation not affecting SMC6 interactions; "−", mutation disrupting all SMC6 complexes; red minus, mutation specifically disrupting the Nse4-SMC6 interaction; the red-highlighted SMC3 amino acids correspond to the Scc1-contacting residues. Amino acid shading represents following conserved amino acids: *dark green*, hydrophobic and aromatic; *light green*, polar; *pink*, basic; *blue*, acidic. Multi-component yeast two-hybrid systems (**B–D**) were employed to determine SMC6 region and residues binding to Nse4. Impact of mutations on the stability of the following SMC6 complexes was tested: SMC6-Nse4-Nse3-Nse1 (**B**), SMC6-Nse4-SMC5 (**C**) and SMC6-Nse5-Nse6 (**D**). Schematic representation of the complexes is at the right side of each panel. (**B**) The full-length hybrid SMC6 and Nse4 constructs were co-transformed together with p416ADH1-Nse1 + Nse3 plasmid into *S. cerevisiae* PJ69 cells. Formation and stability of the SMC6-Nse4-Nse3-Nse1 complex was scored by growth of yeast PJ69 transformants on plates without leucine, tryptophan, uracil and histidine, containing 0.3 mM 3-Amino-1,2,4-triazole (-L,T,U,H, 0.3AT panel). The L964A, L965A, L968A, E969A, L972A and R975A mutations reduce stability of the SMC6 complexes. (**C**) Similarly, the SMC6 and SMC5 were co-transformed together with p416ADH1-Nse4 construct and stability of the SMC5-Nse4-SMC6 complex was scored on plates containing 0.5 mM 3-Amino-1,2,4-triazole (-L,T,U,H, 0.5AT panel). The L964A, L965A, L968A, E969A, L972A and R975A mutations reduce stability of the SMC6 complexes. (**D**) In the control experiment, the same mutations were tested in the SMC6-Nse5-Nse6 complex (constituted of the full-length Gal4AD-SMC6, Gal4BD-Nse5 and non-hybrid Nse6) on plates containing 3 mM 3-Amino-1,2,4-triazole (-L,T,U,H, 3AT panel). The L964A, L968A and E969A mutations affect all SMC6 complexes (**B–D**), while the L965A, L972A and R975A mutations reduce only stability of the SMC6-Nse4 complexes (**B**,**C**), suggesting that the highly conserved L965, L972 and L975 residues are specifically required for the SMC6 interaction with Nse4. Wild-type (WT) or mutant versions of SMC6 are labelled in blue; "−", denotes empty vector control; "+", indicated construct was co-transformed; the Gal4 domain positions are labelled with the black box. Growth of the transformants was verified on the control plates (-L,T,U). All mY2H tests were repeated at least 3 times.

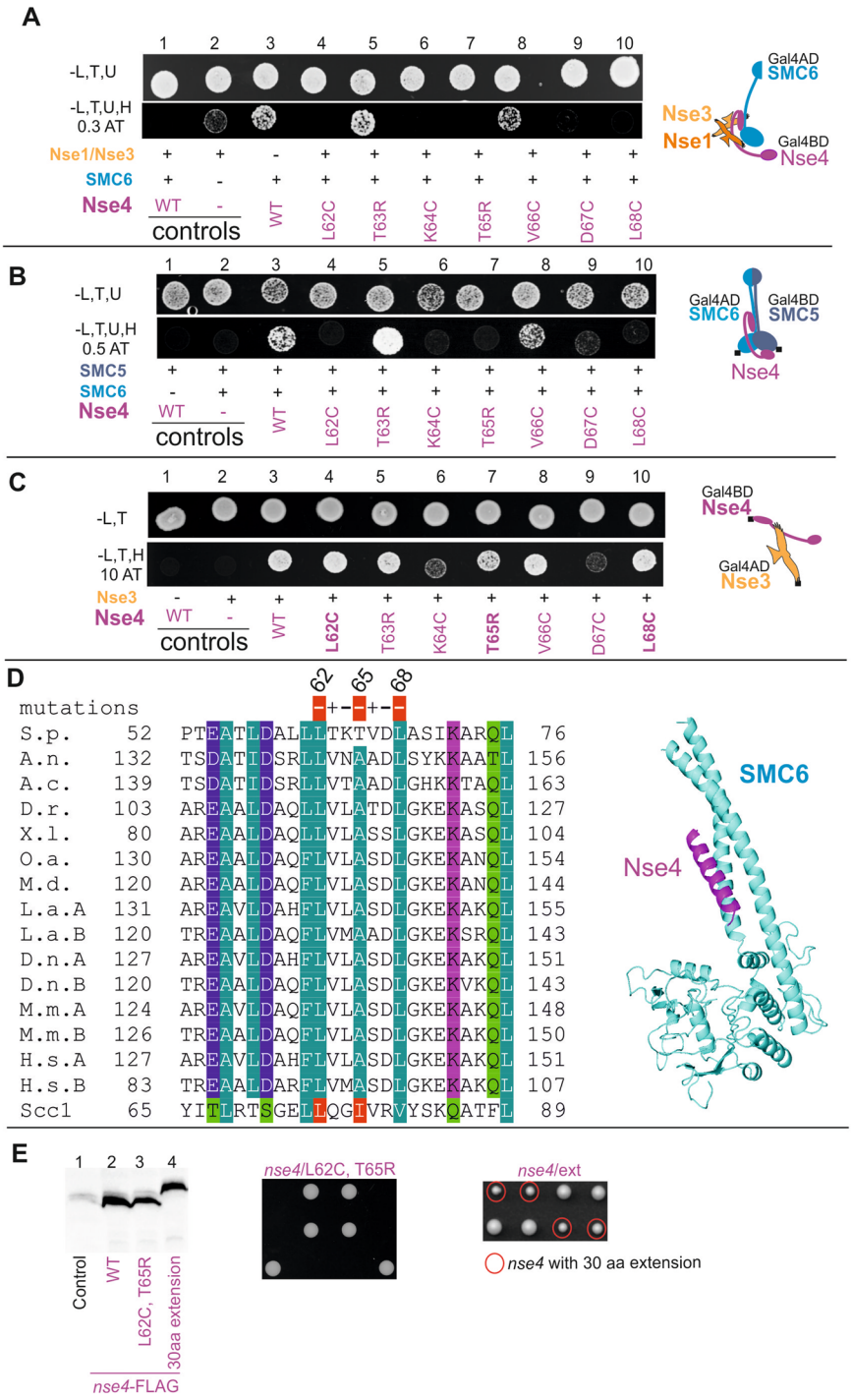

Figure 2. Binding of the Nse4 helix H3 to SMC6 is essential for yeast viability. Identification of the SMC6-binding residues within the Nse4 helix H3 region (aa62-68; **A**–**D**). (**A**) Stability of the SMC6-Nse4-Nse3-Nse1 complex was scored by 4Y2H on the plates containing 0.3 mM 3-Amino-1,2,4-triazole (-L,T,U,H, 0.3 AT panel). (**B**) Stability of the SMC5-Nse4-SMC6 complex was scored by 3Y2H on the plates containing 0.5 mM 3-Amino-1,2,4-triazole (-L,T,U,H, 0.5 AT panel). The Nse4/L62C, K64C, T65R, D67C, and L68C mutations reduce stability of the SMC6-Nse4-Nse3-Nse1 as well as SMC5-Nse4-SMC6 complexes. In the control experiment (**C**), the same mutations were tested for the Nse4-Nse3 interaction in the classical Y2H system (constituted of the full-length Gal4BD-Nse4 and Gal4AD-Nse3). Interactions were scored on plates containing 10 mM 3-Amino-1,2,4-triazole (-L,T,H, 10AT panel). The K64C and D67C mutations affect all Nse4 complexes (**A**–**C**). Intact L62, T65 and L68 Nse4 residues are required specifically for binding to SMC6 (**A**,**B**). Wild-type (WT) or mutant versions of Nse4 are labelled in violet below the panels (further details as in Fig. 1). (**D**) Alignment of the Nse4 helix H3 (of the N-terminal HTH domain). The Scc1 sequence from *S. cerevisiae* represents the kleisin binding mode present in the SMC3-Scc1 crystal structure (PDB: 4UX3). The organisms and figure legends are same as in the Fig. 1A; note that there are two Nse4 genes in the placental mammals denoted as A and B. The SMC6-Nse4 model (right) is based on the protein-protein interaction analysis. (**E**) The Nse4-3xFLAG constructs were

integrated into yeast *S. pombe* diploid cells and the following Nse4 protein levels were compared on western blot (left panel): Nse4/WT (lane2), nse4/ L62C, T65R (lane 3) and Nse4 with 30 amino acids extension of its linker region (lane 4). Tetrad dissection analysis of the *nse4*$^{+}$*/nse4-L62C, T65R* diploid strain shows (middle panel) that the *nse4-L62C, T65R* mutation is lethal, suggesting essential role of the Nse4–SMC6 interaction. The tetrad analysis of the *nse4*$^{+}$*/nse4*^{ext} diploid strain (right panel) suggests growth defect of the *nse4/ext* haploid cells.

affecting multiple Nse4 interactions (e.g. those affecting the Nse4 structure), we tested the Gal4BD-Nse4 mutation constructs in combination with Gal4AD-Nse3 in the classical Y2H system (Fig. 2C)[29,34]. The K64C and D67C mutations affected the Nse3-Nse4 interaction (despite their normal protein levels; Suppl. Fig. S2B), suggesting their deleterious effects on the Nse4 structure (Fig. 2C, columns 6 and 9). In contrast, the other mutations had no effect on the Nse3-Nse4 interaction, suggesting that the intact L62, T65 and L68 conserved residues are required specifically for the Nse4-SMC6 binding (Fig. 2C). Altogether, our data suggest that the Nse4 HTH motif binds the SMC6 neck region and that the SMC6-Nse4 interaction mode is similar to the other νSMC-kleisin interactions[12,13] (Figs. 2D and S2C).

To analyse the role of the Nse4-SMC6 interaction in the fission yeast cells, we introduced the L62C and T65R mutations into the genome of diploid *S. pombe*. In diploid cells, the expression level of the FLAG-tagged nse4/L62C, T65R was comparable to nse4/WT (Fig. 2E, lanes 2 and 3), however, the tetrad analysis showed that the double *nse4-L62C, T65R* mutation was lethal for haploid cells (Fig. 2E, middle panel), suggesting an essential role for the Nse4-SMC6 interaction.

A role for the Nse4 and ATP molecules in bridging of SMC5-SMC6. To compare the role of Nse4 and ATP in bridging of the SMC5-SMC6 heads, we introduced the SMC5/E995Q mutation which inhibits ATP hydrolysis; i.e. enhances ATP retention between SMC5-SMC6 heads and their dimerization (Figs. 3A and S3[14,35]). In the SMC5-Nse4-SMC6 3Y2H system, the interaction between the Gal4BD-SMC5 and Gal4AD-SMC6 constructs was not detectable, suggesting a relatively low stability of the SMC5-SMC6 dimer even upon stable binding of ATP (Fig. 3A, columns 1 and 2). Addition of Nse4 resulted in relatively stable SMC5-Nse4-SMC6 complex formation (Fig. 3A, columns 3 and 4), suggesting that Nse4 stabilizes the bridge between SMC5 and SMC6. The introduction of the ATP-hydrolysis mutation to the SMC5-Nse4-SMC6 complex only slightly increased its relative stability (Fig. 3A, column 4), suggesting a major role of Nse4 (and a minor additive effect of the ATP binding; see below) in bridging of the SMC5-SMC6 heads.

When we reduced the Nse4 binding affinity to SMC6 using the specific Nse4 mutations described above, the stability of the wild-type SMC5 complexes dropped more dramatically than the stability of the SMC5/E995Q mutant complexes (Fig. 3A, compare odd and even columns). For example, the L68C mutation reduced stability of the wild-type SMC5-Nse4-SMC6 complex significantly, while the ATP molecule (in SMC5/E995Q) stabilized the Nse4/L68C complex (Fig. 3A, columns 5 and 6). Further reduction of the Nse4 binding affinity (Fig. 3A, columns 7–12) led to further drops in stability of SMC5-Nse4-SMC6, again, with relatively more stable hydrolytic mutants. Although the stability of the Nse4/L62C, T65R double mutant complex was very low, the residual affinity of Nse4 to SMC6 still supported ATP binding in the SMC5/E995Q mutant (Fig. 3A, columns 11 and 12). These data suggest that ATP contributes significantly to the SMC5-SMC6 bridging when the Nse4 affinity is reduced and that the Nse4 and ATP interactions are synergistic in the SMC5-Nse4-SMC6 complex.

KITE-bound Nse4 is constrained upon ATP binding. To analyse the role of the ATP binding to SMC5-SMC6 within the complex stabilized by the KITE proteins, we added Nse1 and Nse3 to the p416ADH1-Nse4 plasmid (p416ADH1-Nse4 + Nse3 + Nse1 construct, 5Y2H; Fig. 3B[30,36]). Consistent with their Nse4-stabilizing roles (Fig. 1B), the KITE proteins increased the stability of the SMC5-Nse4-SMC6 complex significantly (Fig. 3B, compare columns 1 and 3). Surprisingly, addition of the SMC5/E995Q ATP-hydrolysis mutation greatly destabilized the SMC5-SMC6-Nse4-Nse3-Nse1 complex (Fig. 3B, compare columns 3 and 4), suggesting antagonistic roles of ATP and KITE subunits.

To ensure that the instability of the ATP-bound SMC5-SMC6-Nse4-Nse3-Nse1 complex is specifically caused by the ATP-mediated SMC5-SMC6 head bridge, we introduced either SMC6/S1045R mutation disturbing the ATP-mediated SMC5-SMC6 head dimerization interface or SMC5/K57I mutation abolishing binding of ATP (Suppl. Fig. S3A,B)[14,35,37]. As the SMC6/S1045R mutation suppressed instability caused by the SMC5/E995Q mutation (Suppl. Fig. S3C, column 10), we can exclude a direct impact of this mutation on the SMC5 structure or protein level (Suppl. Fig. S3D). The observation that both mutations suppressed instability caused by the SMC5/E995Q mutation (Suppl. Fig. S3C, column 10 and 12) confirm the notion that the ATP-mediated SMC5-SMC6 head dimerization causes the SMC5-SMC6-Nse4-Nse3-Nse1 instability.

Given that both ATP and Nse4 bridge SMC5-SMC6 heads, our data suggest that the ATP bridge antagonizes the KITE-bound Nse4 bridge (Fig. 3B, compare columns 3 and 4), and vice versa, the KITE-bound Nse4 bridge counteracts the ATP-mediated SMC5-SMC6 dimerization (Fig. 3B, compare columns 2 and 4). To release the constraint imposed by the KITE-bound Nse4 bridge, we reduced the Nse4 binding affinity to SMC6 using the specific Nse4 mutations described above (Figs. 2 and 3A). With reduction of the Nse4 affinity, the relative stability of the ATP-free complexes gradually dropped to its limit (Fig. 3A,B, columns 5, 7, 9 and 11) as the Nse4 bridge was the most dominant one. In contrast, the relative stability of the ATP-bound SMC5-SMC6-Nse4-Nse3-Nse1 complexes dropped first moderately in single mutants (Fig. 3B, columns 6, 8, and 10) and then it partially recovered in the L62C, T65R double mutant (column 12). The relative stability of the single nse4 mutants was less affected in the SMC5/E995Q background (compared to the SMC5/WT background) as the total ATP-bound complex stability was a result of the balance between the competing Nse4 and ATP bridges. In other words, with the weaker

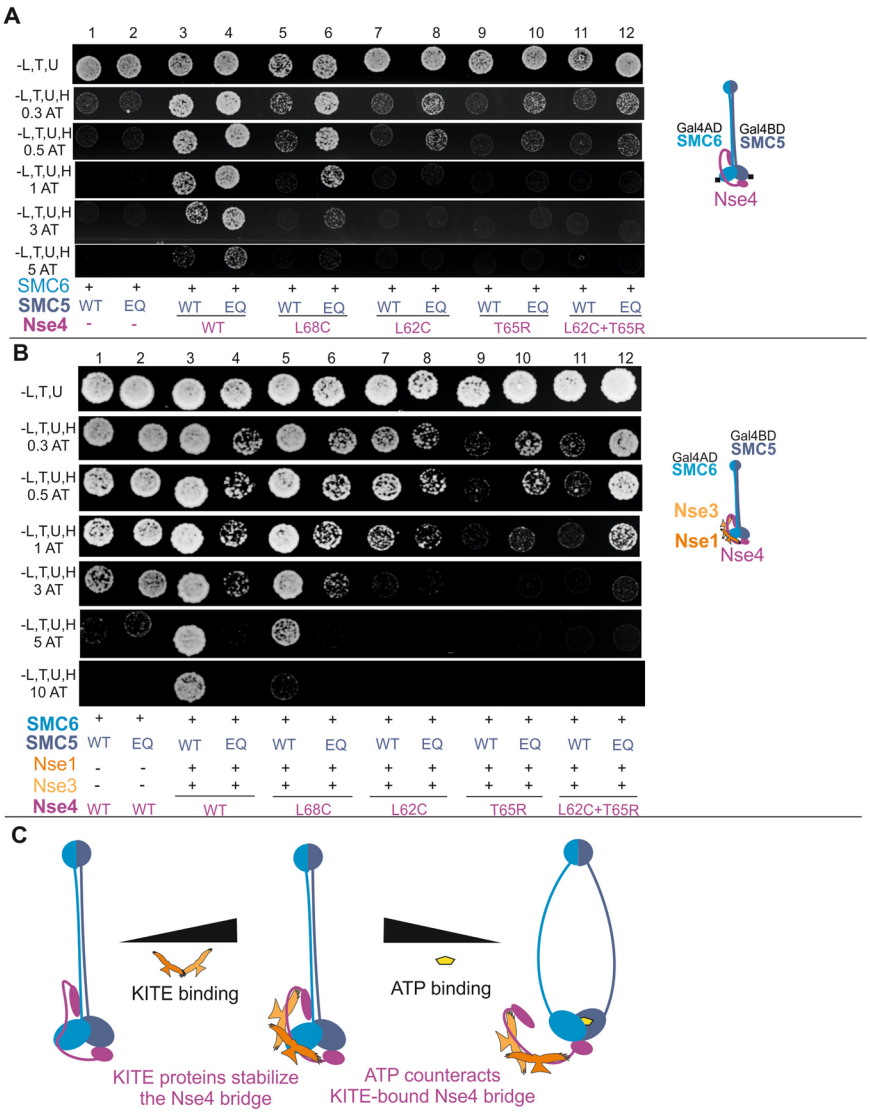

Figure 3. A role of Nse4 and ATP molecules in bridging of SMC5-SMC6. (**A**) Nse4 is essential for the bridging of the hybrid SMC5-SMC6 constructs (columns 1–4). The SMC5/E995 conserved residue was mutated to glutamine (EQ) to inhibit ATP hydrolysis. The ATP retention has only mild additive effect on the stability of the SMC5-Nse4-SMC6 complex (scored on plates containing increasing concentrations of 3-Amino-1,2,4-triazole). The Nse4 mutations affect the stability of the wild-type SMC5 complexes more dramatically than the stability of the SMC5/E995Q mutant complexes (compare odd and even columns). Wild-type (WT) or E995Q (EQ) mutant versions of SMC5 are labelled in grey below the panels (further details as in Figs. 1 and 2). (**B**) Addition of the Nse1 and Nse3 KITE proteins to the above SMC5/SMC6/Nse4 system stabilizes the SMC5-Nse4-SMC6 bridge. Although the KITE proteins stabilize the ATP-free SMC5-Nse4-SMC6 complex (columns 1 and 3), they destabilize the ATP-bound complex (columns 2 and 4). The Nse4 mutations decrease stability of the ATP-free SMC5-SMC6-Nse4-Nse3-Nse1 complex gradually (columns 5, 7, 9 and 11), while the stability of the ATP-bound complexes drops first (columns 6, 8, and 10) and then it recovers in the L62C, T65R double mutant (column 12). (**C**) Schematic summary of the panel A and B results showing the stabilizing effect of the KITE binding to the Nse4 bridge and the destabilizing effect of ATP to the KITE-bound Nse4 bridge. The ATP-imposed constraint is partially released via dissociation of the Nse4-SMC6 interaction.

Nse4 binding (and therefore lower complex stability), there was a weaker ATP-mediated constraint which allowed better ATP binding and improved complex stability. In the L62C, T65R double mutant, when the Nse4-SMC6 interaction was very weak, the ATP binding was only weakly opposed by the KITE-bound Nse4 bridge and ATP could bridge the SMC5-SMC6 heads efficiently (column 12).

Altogether, these data suggest that ATP constrains KITE-bound Nse4 bridge and vice versa, the KITE-bound Nse4 bridge counteracts the ATP-mediated SMC5-SMC6 heads dimerization, and that this constraint might be released via dissociation of the Nse4-SMC6 interaction (Fig. 3C).

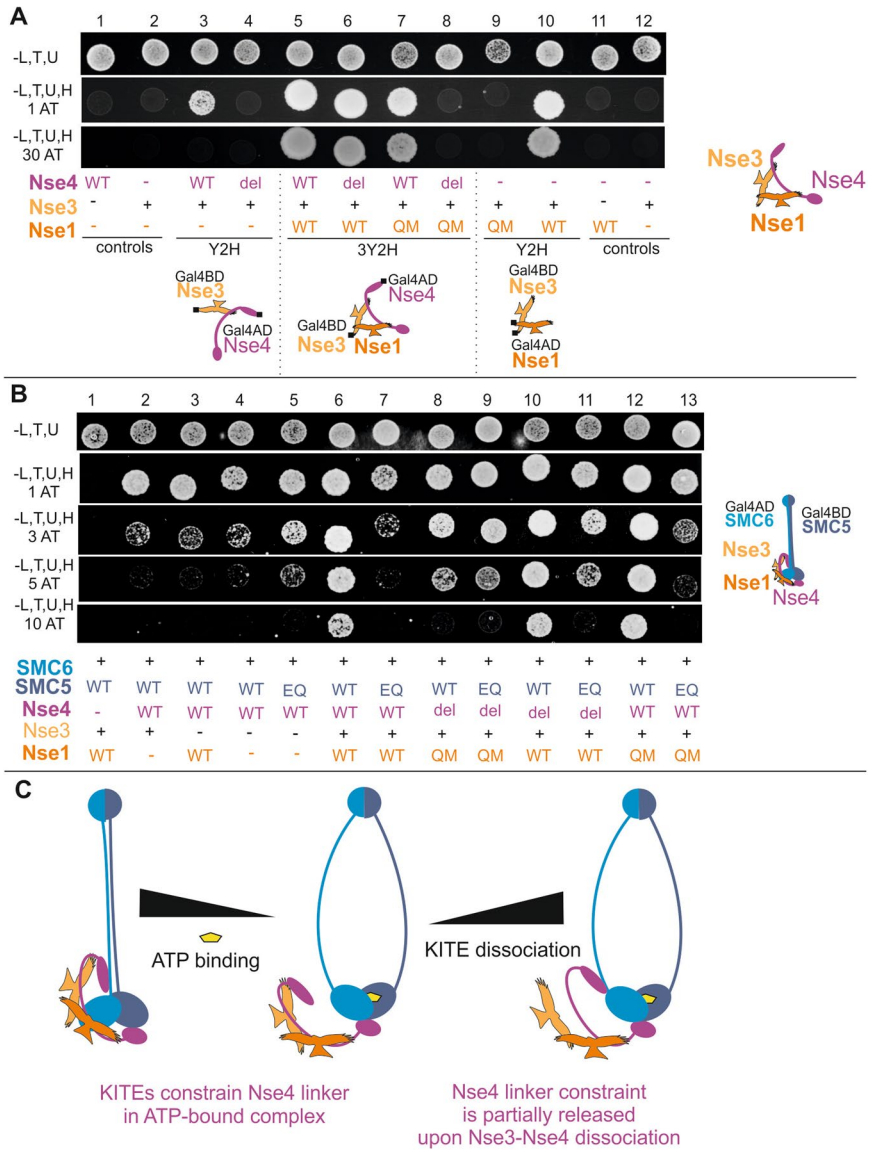

Figure 4. The KITE proteins constrain the Nse4 kleisin linker. (**A**) The Nse1-Nse3-Nse4 subcomplex is held by mutual interactions between its subunits. The Nse4/del87-91 (del) deletion disturbs the Nse3-Nse4 binary interaction (columns 3 and 4) and the Nse1/Q18A, M21A (QM) mutation abrogates the Nse1-Nse3 binary interaction (columns 9 and 10), but they do not alter stability of the Nse1-Nse3-Nse4 trimer individually (columns 6 and 7). However, combination of these two mutations reduces the stability of Nse1-Nse3-Nse4 significantly (column 8). (**B**) The combination of the Nse4/del87-91 and Nse1/Q18A, M21A mutations compromises the stability of the wild-type SMC5-SMC6-Nse4-Nse3-Nse1 complex (compare columns 6 and 8), but increases the stability of the ATP-bound complex (compare columns 7 and 9). Notably, there is no difference between stability of the ATP-free and ATP-bound complexes (compare columns 8 and 9), suggesting that the binding of the KITE proteins to Nse4 destabilizes the ATP-bound complexes. Furthermore, the Nse4/del87-91 mutation alone also partially supresses the instability of the ATP-bound complex (column 11), suggesting that the binding of Nse3 to Nse4 linker constrains the linker. (**C**) Schematic summary of the results showing the constraint effect of ATP (Fig. 3) and its partial release via dissociation of the Nse3-Nse4 interaction.

The ATP-mediated constraint depends on the KITE subunits. In the SMC5/6 complex, the KITE and kleisin subunits form a tight Nse1-Nse3-Nse4 sub-complex mediated by their mutual interactions (Fig. 4A)[28,34]. As ATP constrained the Nse4 bridge only in the presence of the KITE subunits (Fig. 3A,B, columns 3 and 4), we introduced mutations specifically affecting the stability of the Nse1-Nse3-Nse4 trimer to evaluate a role of the KITE proteins. Specific mutations disturbing only individual Nse1-Nse3 (Nse1/Q18A, M21A) and Nse3-Nse4 (Nse4/del87–91) binary interactions (Fig. 4A, compare columns 3 against 4 and 9 against 10) did not affect the stability of the whole Nse1-Nse3-Nse4 trimer (Fig. 4A, columns 6 and 7), but their combination compromised trimer assembly (Fig. 4A, column 8). When we introduced this combination of Nse1 and Nse4 mutations to the SMC5-SMC6-Nse4-Nse3-Nse1 complex, its stability was reduced as the KITE proteins lost their ability to bind

and stabilize Nse4 (Fig. 4B, compare columns 6 and 8). In contrast, when we introduced this combination of Nse1 and Nse4 mutations to the SMC5/E995Q hydrolytic mutant complex, the stability of the ATP-bound complex was increased (Fig. 4B, compare columns 7 and 9), suggesting that the ATP-induced constraint of Nse4 depends on its binding to the KITE subunits. Importantly, there was no difference between the stability of the ATP-free and ATP-bound complexes (compare columns 8 and 9), further corroborating our conclusion that the ATP-mediated constraint depends on the binding of the KITE dimer to Nse4. Furthermore, the Nse4/del87-91 mutation compromising only Nse3-Nse4 interaction (Fig. 4A, columns 4 and 6) had a suppressing effect on the SMC5/E995Q complex similar to the double mutant (Fig. 4B, compare columns 9 and 11), suggesting that the binding of Nse3 to the Nse4 linker partially constrained it. Our data suggest that the instability of the SMC5/6 core complex induced by the ATP binding is dependent on the binding of KITE proteins to the Nse4 kleisin linker and that the constraint can be partially released via dissociation of the Nse3-Nse4 interaction (Fig. 4C).

The limited size of the Nse4 linker imposes mechanical constraint. The KITE dimers bind the linker regions of kleisin molecules in the SMC complexes (Fig. 5A)[7,16,29,38–40]. To explore the role of the Nse4 linker in propagation of the ATP-induced constraint, we inserted a 30 amino acid extension at the putative end of the linker (Figs. 5A and S4A) to lengthen the linker. The Nse4 extended construct bound the Nse1-Nse3 KITE proteins normally (Fig. 5A) and formed the SMC5-SMC6-Nse4-Nse3-Nse1 complex with the relative stability similar to that with the normal Nse4 construct (Fig. 5B, columns 3 and 4). Interestingly, combination of the Nse4 extended construct with the SMC5/E995Q ATP-hydrolysis mutant partially increased the relative stability of the SMC5-SMC6-Nse4-Nse3-Nse1 complex, suggesting that the extended Nse4 linker partially alleviated the ATP-induced constraint (Fig. 5B, columns 5 and 6).

To assess the importance of the Nse4 linker size and the effect of its extension, we also introduced the 30 amino acid extension into the genomic copy of the fission yeast Nse4. In yeast diploid cells, the expression level of the FLAG-tagged nse4/ext was comparable to nse4/WT (Fig. 2E, lanes 2 and 4), however, the tetrad analysis showed that the haploid cells were sick (Fig. 2E, right panel). In addition, the *nse4/ext* haploid cells exhibited severe hydroxyurea (HU) and methyl methane sulfonate (MMS) sensitivities similar to that of the *smc6-74* hypomorphic mutant (Fig. 5C), suggesting an important role of the Nse4 linker size for the SMC5/6 function during DNA repair and replication.

Discussion

The kleisin subunits bridge the SMC heads in an asymmetric way and lock the SMC ring at its head side[12,13,16,18]. We have shown that Nse4 belongs to the kleisin superfamily of proteins and binds strongly to the κSMC5 head via its Nse4 C-terminal WHD[28]. However, we observed only weak binding of Nse4 to νSMC6 (Fig. S1A)[28] and other studies actually failed to show the Nse4-SMC6 interaction[31,32,41]. Here we developed several unique systems to prove and analyse the interaction between Nse4 and SMC6. We mapped the Nse4-SMC6 interface in detail and found that the Nse4-SMC6 interaction mode is similar to the other νSMC-kleisin interactions (Figs. 2 and S2C[16–18,25,27]). Therefore, we assume that Nse4 bridges the SMC5-SMC6 proteins in a way similar to kleisins in the other SMC complexes, except that the Nse4 bridge is specifically modulated by the Nse1-Nse3 KITE subunits in the SMC5/6 complex (see below).

The kleisins lock the SMC rings that can embrace DNA or extrude a loop in an ATP-dependent way[42,43]. To release such entrapped DNA, the SMC-SMC or SMC-kleisin interface must be open. It was proposed that the νSMC-kleisin interface opens and serves as an exit gate for trapped DNA[19,44,45]. In the cohesin complex, the Scc1-SMC3 interface is opened upon ATP binding (in the presence of the Pds5 and Wapl regulators[19–24]). Our data show that the SMC5/6 core complex is relatively less stable in the ATP-bound state than in the ATP-free state, suggesting that one or more protein-protein interaction interfaces are compromised upon ATP binding (Fig. 5D). Given the weak nature of the Nse4-SMC6 interaction, we assume that this interaction is prone to dissociation and that the Nse4-SMC6 interface is opened upon ATP binding. Consistent with the latter notion, the ATP-mediated constraint was released when the Nse4-SMC6 interaction was disturbed (Fig. 3B). Therefore, we hypothesize that the binding of ATP to the SMC5-SMC6 heads constrains the Nse4 bridge (when bound by the Nse1 and Nse3 KITE subunits; see below and Fig. 5D) and this constraint is partially released via dissociation of the Nse4-SMC6 interaction.

The ATP binding induces changes in the mutual positions (and conformations) of the SMC heads and arms[10,27,46–48]. Consequently, the shape of the whole SMC complex changes from a rod-like conformation (with juxtaposed arms stabilized by their mutual interactions) to the less stable open ring (Fig. 5D). As for the other SMC complexes, we hypothesize that at least part of the ATP-induced SMC5/6 instability (Fig. 5D) might be a consequence of such SMC-SMC shape transition from the rod to ring. However, we observed this instability only in the presence of the KITE subunits, suggesting that either our system is unable to detect the SMC5-SMC6 rod-to-ring shape transition (and monitors only Nse4 bridge opening) or the KITE proteins are required for the full rod-to-ring shape transition. The latter possibility is consistent with the prokaryotic SMC/ScpAB data which suggest an important function of the KITE subunits in pulling SMC arms[26,27]; however, further experiments with purified SMC5/6 complexes are needed to resolve this issue. In our hypothetical model, the binding of ATP to the SMC5-SMC6 heads pulls their arms apart and constrains the KITE-bound Nse4 bridge (Fig. 5D).

It was shown that kleisin-interacting proteins (particularly KITE and HAWK subunits) bind and shape linker regions of the kleisin molecules[7,11,16,29,38–40,49–51]. Our data showed that the binding of the Nse1-Nse3 KITE dimer increases the Nse4 ability to bind SMC5-SMC6 subunits in ATP-free state (Figs. 3B and 4B), suggesting that the KITE binding may stabilize and shape Nse4 to fit the ATP-free conformation of the SMC5/6 core complex. In contrast, the KITE-bound Nse4 linker is less compatible with the ATP-bound conformation of SMC5/6. Consistent with these notions, extensions of the Nse4 linker partially relaxed its stiff shape and resulted in the reduced stability of the ATP-free complexes (Figs. 5B and S4). On the contrary, the linker extensions partially released the

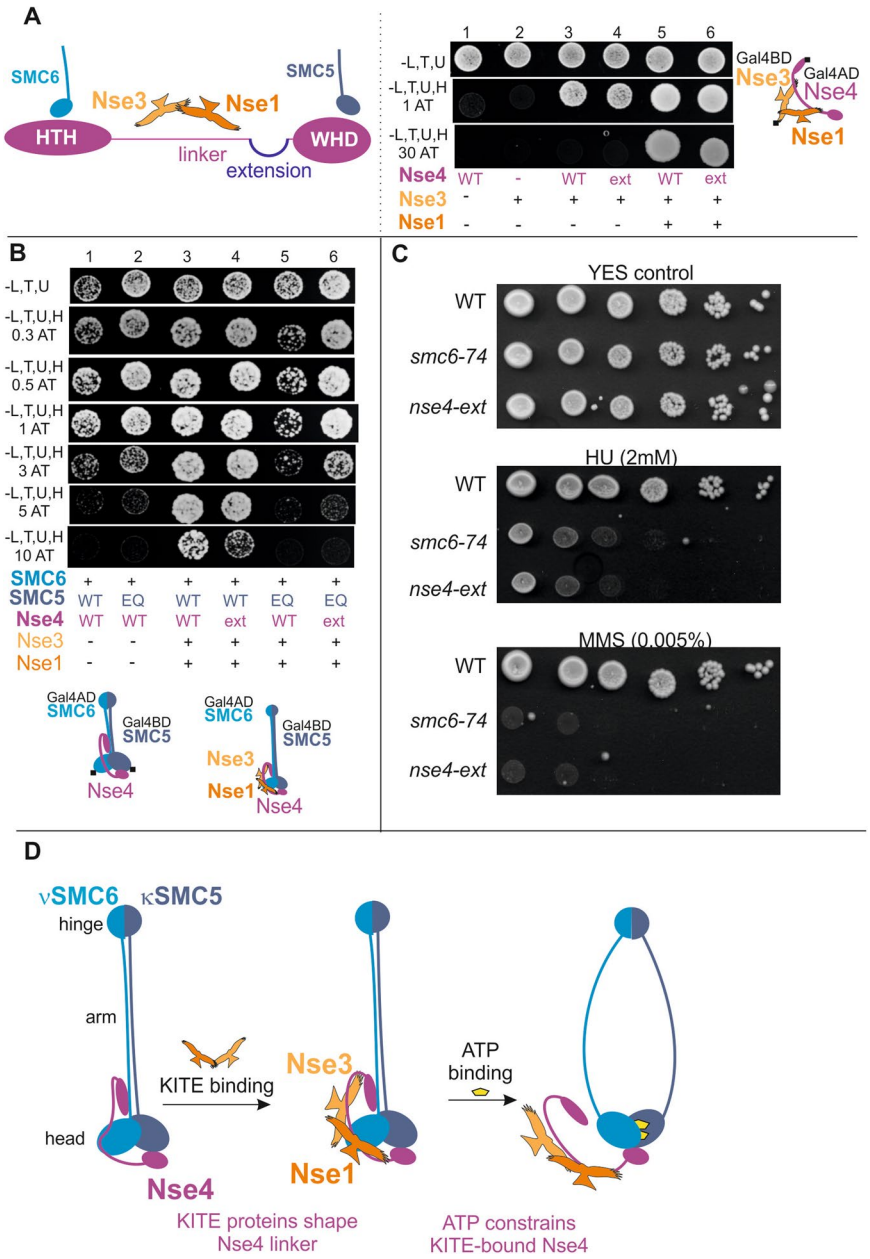

Figure 5. The limited size of the Nse4 linker poses mechanical constraint. (**A**) Schematic representation (left panel) of the Nse4 regions with their binding partners (depicted above). The 30 amino acid extension is inserted at the end of the linker (after aa174; Suppl. Fig. S4A). In the control experiments (right panel), the 30 amino acid extension (ext) does not affect the stability of either Nse3-Nse4 binary interaction (column 4) or Nse1-Nse3-Nse4 trimer (column 6). (**B**) The stability of the ATP-free SMC5-SMC6-Nse4-Nse3-Nse1 complex containing nse4/WT or nse4/ext is comparable (columns 3 and 4), while the extension of the linker results in the partial relief of the ATP-induced tension in the SMC5/E995Q complex (compare columns 5 and 6). (**C**) The *S. pombe smc6-74* and *nse4/ext* hypomorphic mutants were tested for sensitivity to hydroxyurea (HU) or methyl methane sulfonate (MMS) using tenfold serial dilutions. (**D**) The schematic summary of the roles of the KITE subunits in the ATPase cycle of SMC5/6. Our data show that the SMC5/6 core complex is less stable in the ATP-bound state than in the ATP-free state. We hypothesize that the KITE-shaped Nse4 linker fits the ATP-free conformation of SMC5/6 (and therefore increases its stability), while the ATP-bound conformation is less compatible with the KITE-shaped Nse4 linker (and therefore constrains the Nse4 bridge). The reduced stability of the ATP-bound complex may suggest that one or more protein-protein interaction interfaces are compromised upon ATP binding. The results in the Fig. 3 suggest that the Nse4-SMC6 interface might be open. The results in the Fig. 4 also point to the Nse4-Nse3 interface. In addition, the interface between SMC5-SMC6 arms might be disturbed upon the ATP binding as suggested for the other SMC complexes. The stiff KITE-bound Nse4 linker may transduce a pulling force generated by the binding of ATP to the SMC5-SMC6 heads. In consequence, the Nse4-SMC6 and Nse4-Nse3 interfaces may open and release the Nse4 constraint.

ATP-induced constraint in the ATP-bound complexes. Therefore, we suggest that the KITE subunits shape the Nse4 linker to fit the ATP-free complex optimally and to facilitate opening of the complex upon ATP binding (Fig. 5D). Consistent with this conclusion, the ATP-mediated constraint was partially suppressed upon release of the part of the Nse4 linker from the Nse3 binding pocket (Fig. 4B)[29,34]. Altogether, we hypothesize that the Nse4 linker is stiffened upon its KITE binding and transduces a pulling force generated by the binding of ATP to the SMC5-SMC6 heads (Fig. 5D). In consequence, the Nse4-SMC6 interface opens and releases the Nse4 constraint.

Similarly, it was proposed that binding of the HAWK (Scc3 and Pds5) and Wapl proteins to the Scc1 kleisin stiffens its linker region and transduces conformational energy of the ATP-dependent SMC head dimerization to the dissociation of Scc1 from Smc3[19,45]. In the absence of the Pds5-Wapl regulators, the cohesin's head movements driven by the ATP binding and hydrolysis cannot be effectively coupled to exit gate opening as the Scc1 linker is flexible. Interestingly, the size of the Scc1 linker is much longer (cca 400 amino acids) than the size of the Nse4 linker). Accordingly, the Scc3 HAWK subunit covers only a small part of the Scc1 linker and requires Pds5-Wapl regulators to shape the long Scc1 linker, while the KITE subunits are sufficient to shape their short kleisin partners[27,38]. As mentioned above, the extension of the Nse4 linker region suppressed the ATP-induced constraint, suggesting that the short size of the Nse4 linker is critical for the dynamics of the SMC5/6 complex (Figs. 5 and S4D). Consistent with this notion, the integration of the 30 amino acid long extension to the genomic copy of the fission yeast Nse4 resulted in the severe DNA repair phenotypes (Fig. 5C).

Taken together, we propose a hypothetical model in which the KITE proteins shape the kleisin linker connecting the SMC heads (Fig. 5D). The KITE-shaped Nse4 linker fits the ATP-free conformation of SMC5/6 (and therefore increases its stability), while the ATP-bound conformation is less compatible with the KITE-shaped Nse4 linker (and therefore constrains the Nse4 bridge). This hypothetical model suggests a key role of the kleisin and KITE subunits in the molecular mechanisms driving the SMC5/6 dynamics.

Material and Methods

Plasmids. Most of the Y2H constructs were prepared previously: pGBKT7-Nse3(aa1-328), pGADT7-Nse3(aa1-328) and pGBKT7-Nse4(aa1-300) constructs were created in[33], pOAD-Nse1(aa1-232) was created in[34], pGADT7-SMC6 (aa1-1140) was described in[36]. To generate pGBKT7-SMC5(aa1-1076) construct, the yeast *S. pombe* SMC5 cDNA was PCR amplified by oLV511 + oLV486 (Supplementary Table 2) and inserted into the *NcoI–SalI* digested pGBKT7 by In-Fusion cloning protocol (Clontech, USA). Nse5 was cloned into pGBKT7 vector using *NcoI* and *SalI* sites and classical T4 ligase protocol.

To create the pGADT7-Nse4(aa1-300)/WT, pGADT7-Nse4(aa1-300)/del87-91 and pGADT7-Nse4(aa1-300)/ext constructs, Nse4 was PCR amplified from the corresponding p416ADH1-Nse4 plasmids (see below) by oLV575 + oLV576 and inserted into *NdeI-BamHI* digested pGADT7 by In-Fusion cloning protocol.

Multicomponent Y2H system was described in the protocol book series Methods in Molecular Biology[30]. The p416ADH1-Nse1(aa1–232) construct was created previously[34]. Construction of p416ADH1-Nse4 (aa1-300), p416ADH1-Nse3(aa1–328) + Nse4(aa1–300) and p416ADH1-Nse3(aa1–328) + Nse4(aa1–300) + Nse1(aa1–232) was described previously[30,36] (the vector name pPM587 equals to p416ADH1). p416ADH1-Nse4(aa1–300) + Nse1(aa1–232) and p416ADH1-Nse3(aa1–328)+Nse1(aa1–232) were prepared by PCR-amplification of ADH1-Nse1(1-232)-CYC terminator from p416ADH1-Nse1 by KB353 + KB354 and its insertion into *KpnI* digested p416ADH1-Nse4 (aa1-300) and p416ADH1-Nse3(aa1–328) by In-Fusion protocol, respectively. The p416ADH1-Nse6(1-522) construct was prepared using PCR-amplification of Nse6 by EB77 + EB78 primers and insertion into *SalI-SpeI* digested p416ADH1 by In-Fusion protocol.

To prepare p416ADH1-Nse4/ext, *SalI* restriction site in the p416ADH1 multi-cloning site (MCS) was mutated by site-directed mutagenesis (SDM; see below) with oLV522 + oLV523 (Suppl. Table 3). Then, *SalI* site was inserted by SDM behind the aa174 with oLV520 + oLV521. This construct was *SalI* digested, $(G_4S)_6$ linker was amplified by oLV579 + oLV580 and inserted using the In-Fusion cloning protocol.

Construct for the *S. pombe* genome integration was prepared as follows: 1. Nse4 was cloned within the *BamHI* and *EcoRI* sites of the pSK-ura4 plasmid; 2. genomic sequence downstream of the Nse4 gene was PCR amplified (JP414 and JP415) and inserted to the pGEM-Easy vector (Promega, USA); 3. The *SacI-SalI* fragment of the pSK-Nse4-ura4 plasmid was inserted to the *SacI-XhoI* digested pGEM-3′end construct to get the pGEM-Nse4(WT)-ura4 integration plasmid. To create pGEM-Nse4(L62C, T65R)-ura4 and pGEM-Nse4/ext, the Nse4 sequences were PCR amplified from the p416ADH1-Nse4 constructs by oLV680 + oLV681 (Supplementary Table 2) and inserted into *BamHI-EcoRI* digested pGEM-Nse4(WT)-ura4 integration construct by the In-Fusion cloning protocol. Additionally, the *Nde*I site was introduced next to the Nse4 ORF (using oLV689 + oLV690 primers for SDM) and three copies of FLAG-tag (amplified by oLV691 + oLV692 primers) were inserted to the *Nde*I site.

Site-directed mutagenesis. The QuikChange Lightning Site-Directed Mutagenesis Kit (Agilent Technologies, USA) was used to create mutations in pGBKT7-SMC5, pGADT7-SMC6, p416ADH1-Nse4, p416ADH1-Nse3 + Nse4 + Nse1, pGADT7-Nse4, pOAD-Nse1, p416ADH1-Nse1, and pGEM-Nse4. The sequences of primers used for mutagenesis are listed in the Supplementary Table 3.

Yeast two-hybrid assays. The Gal4-based Y2H system was used to analyse *S. pombe* SMC5/6 complex interactions (detailed protocols are described in the book series Methods in Molecular Biology[30]). Briefly, three plasmids pGBKT7, pGADT7 and p416ADH1 with corresponding genes were co-transformed into the *Saccharomyces cerevisiae* PJ69–4a strain and selected on SD -Leu, -Trp, -Ura plates. Drop tests were carried out on SD -Leu, -Trp, -Ura, -His (with 0; 0.3; 0.5; 1; 2; 3; 4; 5; 10; 15; 20; 30 mM 3-aminotriazole) plates at 28 °C. Each combination was co-transformed at least three times and at least three independent drop tests were carried out.

Generation and phenotyping of *nse4* mutant strains of *S. pombe*. Standard genetic techniques were used for preparation of fission yeast *S. pombe* diploid strain by crossing *ade6-M216* strain with *ade6-M210*[52]. The pGEM-Nse4-3xFLAG-ura4 wild-type or mutant integration constructs (digested by *Not*I) were transformed into the diploid strain and the transformants were selected on –ura –ade plates. Using standard genetic techniques, spores of the *nse4+/nse4-mutant* strains were generated and dissected.

S. pombe cultures were grown to mid-log phase, concentrated to 3×10^7 cells/ml, and serial 10-fold dilutions were spotted onto rich media with indicated dose of DNA-damaging agent. Subsequently, plates were incubated at 28 °C for 3 days.

Protein expression analysis. Yeast cells were grown to OD~2.5 and lysed by incubation in 0.1 M NaOH for 5 min and boiling in SDS Laemmli buffer (0.06 M Tris–HCl, pH 6.8, 2% SDS, 4% β-mercaptoethanol, 0.0025% bromophenol blue[53]). Samples were separated by 10% SDS-PAGE and immunoblotted with anti-FLAG-M2-HRP (Sigma Aldrich – A8592) antibody.

Protein modelling. The I-TASSER suite[54] was used to model SMC6 and Nse4 proteins (based on the SMC3-Scc1 crystal structure 4UX3). These protein partners were docked using HADDOCK tool[55] and their specific contact residues (identified in the Figs. 1 and 2, respectively) were used as the docking restrains. The SMC6-Nse4 model most similar to the SMC3-Scc1 crystal structure (4UX3) was selected using the COZOID tool[56,57].

Received: 2 October 2019; Accepted: 20 May 2020;
Published online: 16 June 2020

References

1. Schwarzer, W. *et al.* Two independent modes of chromatin organization revealed by cohesin removal. *Nature* **551**, 51–56, https://doi.org/10.1038/nature24281 (2017).
2. Kschonsak, M. & Haering, C. H. Shaping mitotic chromosomes: From classical concepts to molecular mechanisms. *Bioessays* **37**, 755–766, https://doi.org/10.1002/bies.201500020 (2015).
3. Aragon, L. In *Annual Review of Genetics*, *Vol 52* Vol. 52 *Annual Review of Genetics* (ed. Bonini, N. M.) 89–107 (Annual Reviews, 2018).
4. Palecek, J. J. SMC5/6: Multifunctional Player in Replication. *Genes* **10**, E7, https://doi.org/10.3390/genes10010007 (2019).
5. Bürmann, F. & Gruber, S. SMC condensin: promoting cohesion of replicon arms. *Nat. Struct. Mol. Biol.* **22**, 653–655, https://doi.org/10.1038/nsmb.3082 (2015).
6. van der Crabben, S. N. *et al.* Destabilized SMC5/6 complex leads to chromosome breakage syndrome with severe lung disease. *J. Clin. Investigation* **126**, 2881–2892, https://doi.org/10.1172/jci82890 (2016).
7. Palecek, J. J. & Gruber, S. Kite Proteins: a Superfamily of SMC/Kleisin Partners Conserved Across Bacteria, Archaea, and Eukaryotes. *Structure* **23**, 2183–2190, https://doi.org/10.1016/j.str.2015.10.004 (2015).
8. Wells, J. N., Gligoris, T. G., Nasmyth, K. A. & Marsh, J. A. Evolution of condensin and cohesin complexes driven by replacement of Kite by Hawk proteins. *Curr. Biol.* **27**, R17–R18, https://doi.org/10.1016/j.cub.2016.11.050 (2017).
9. Burmann, F. *et al.* Tuned SMC Arms Drive Chromosomal Loading of Prokaryotic Condensin. *Mol. Cell* **65**, 861–+, https://doi.org/10.1016/j.molcel.2017.01.026 (2017).
10. Diebold-Durand, M. L. *et al.* Structure of Full-Length SMC and Rearrangements Required for Chromosome Organization. *Mol. Cell* **67**, 334–347.e335, https://doi.org/10.1016/j.molcel.2017.06.010 (2017).
11. Nasmyth, K. & Haering, C. H. The structure and function of SMC and kleisin complexes. *Annu. Rev. Biochem.* **74**, 595–648 (2005).
12. Hassler, M., Shaltiel, I. A. & Haering, C. H. Towards a Unified Model of SMC Complex Function. *Curr. Biol.* **28**, R1266–R1281, https://doi.org/10.1016/j.cub.2018.08.034 (2018).
13. Gligoris, T. & Löwe, J. Structural Insights into Ring Formation of Cohesin and Related Smc Complexes. *Trends Cell Biol.* **26**, 680–693, https://doi.org/10.1016/j.tcb.2016.04.002 (2016).
14. Lammens, A., Schele, A. & Hopfner, K. P. Structural biochemistry of ATP-driven dimerization and DNA-stimulated activation of SMC ATPases. *Curr. Biol.* **14**, 1778–1782 (2004).
15. Arumugam, P. *et al.* ATP hydrolysis is required for cohesin's association with chromosomes. *Curr. Biol.* **13**, 1941–1953 (2003).
16. Bürmann, F. *et al.* An asymmetric SMC-kleisin bridge in prokaryotic condensin. *Nat. Struct. Mol. Biol.* **20**, 371–379, https://doi.org/10.1038/nsmb.2488 (2013).
17. Gligoris, T. G. *et al.* Closing the cohesin ring: structure and function of its Smc3-kleisin interface. *Science* **346**, 963–967, https://doi.org/10.1126/science.1256917 (2014).
18. Zawadzka, K. *et al.* MukB ATPases are regulated independently by the N- and C-terminal domains of MukF kleisin. *Elife* **7**, https://doi.org/10.7554/eLife.31522 (2018).
19. Murayama, Y. & Uhlmann, F. DNA Entry into and Exit out of the Cohesin Ring by an Interlocking Gate Mechanism. *Cell* **163**, 1628–1640, https://doi.org/10.1016/j.cell.2015.11.030 (2015).
20. Beckouët, F. *et al.* Releasing Activity Disengages Cohesin's Smc3/Scc1 Interface in a Process Blocked by Acetylation. *Mol. Cell* **61**, 563–574, https://doi.org/10.1016/j.molcel.2016.01.026 (2016).
21. Buheitel, J. & Stemmann, O. Prophase pathway-dependent removal of cohesin from human chromosomes requires opening of the Smc3-Scc1 gate. *EMBO J.* **32**, 666–676, https://doi.org/10.1038/emboj.2013.7 (2013).
22. Eichinger, C. S., Kurze, A., Oliveira, R. A. & Nasmyth, K. Disengaging the Smc3/kleisin interface releases cohesin from Drosophila chromosomes during interphase and mitosis. *EMBO J.* **32**, 656–665, https://doi.org/10.1038/emboj.2012.346 (2013).
23. Chan, K. L. *et al.* Cohesin's DNA exit gate is distinct from its entrance gate and is regulated by acetylation. *Cell* **150**, 961–974, https://doi.org/10.1016/j.cell.2012.07.028 (2012).
24. Elbatsh, A. M. O. *et al.* Cohesin Releases DNA through Asymmetric ATPase-Driven Ring Opening. *Mol. Cell* **61**, 575–588, https://doi.org/10.1016/j.molcel.2016.01.025 (2016).
25. Hassler, M. *et al.* Structural Basis of an Asymmetric Condensin ATPase Cycle. *Mol. Cell* **74**, 1175–1188.e1179, https://doi.org/10.1016/j.molcel.2019.03.037 (2019).
26. Minnen, A. *et al.* Control of Smc Coiled Coil Architecture by the ATPase Heads Facilitates Targeting to Chromosomal ParB/parS and Release onto Flanking DNA. *Cell Rep.* **14**, 2003–2016, https://doi.org/10.1016/j.celrep.2016.01.066 (2016).
27. Kamada, K., Su'etsugu, M., Takada, H., Miyata, M. & Hirano, T. Overall Shapes of the SMC-ScpAB Complex Are Determined by Balance between Constraint and Relaxation of Its Structural Parts. *Structure* **25**, 603–616.e604, https://doi.org/10.1016/j.str.2017.02.008 (2017).

28. Palecek, J., Vidot, S., Feng, M., Doherty, A. J. & Lehmann, A. R. The SMC5-6 DNA repair complex: Bridging of the SMC5-6 heads by the Kleisin, NSE4, and non-Kleisin subunits. *J. Biol. Chem.* **281**, 36952–36959 (2006).
29. Guerineau, M. *et al*. Analysis of the Nse3/MAGE-Binding Domain of the Nse4/EID Family Proteins. *Plos one* **7**, e35813 (2012).
30. Paleček, J. J., Vondrová, L., Zábrady, K. & Otočka, J. Multicomponent Yeast Two-Hybrid System: Applications to Study Protein-Protein Interactions in SMC Complexes. *Methods Mol. Biol.* **2004**, 79–90, https://doi.org/10.1007/978-1-4939-9520-2_7 (2019).
31. Duan, X. *et al*. Architecture of the Smc5/6 Complex of Saccharomyces cerevisiae Reveals a Unique Interaction between the Nse5-6 Subcomplex and the Hinge Regions of Smc5 and Smc6. *J. Biol. Chem.* **284**, 8507–8515 (2009).
32. Diaz, M. *et al*. SMC5/6 Complex Subunit NSE4A is Involved in DNA Damage Repair and Seed Development in Arabidopsis. *Plant Cell*, https://doi.org/10.1105/tpc.18.00043 (2019).
33. Sergeant, J. *et al*. Composition and architecture of the Schizosaccharomyces pombe Rad18 (Smc5-6) complex. *Mol. Cell Biol.* **25**, 172–184 (2005).
34. Hudson, J. J. R. *et al*. Interactions between the Nse3 and Nse4 Components of the SMC5-6 Complex Identify Evolutionarily Conserved Interactions between MAGE and EID Families. *Plos one* **6**, https://doi.org/10.1371/journal.pone.0017270 (2011).
35. Kanno, T., Berta, D. G. & Sjögren, C. The Smc5/6 Complex Is an ATP-Dependent Intermolecular DNA Linker. *Cell Rep.* **12**, 1471–1482, https://doi.org/10.1016/j.celrep.2015.07.048 (2015).
36. Zabrady, K. *et al*. Chromatin association of the SMC5/6 complex is dependent on binding of its NSE3 subunit to DNA. *Nucleic Acids Res.* **44**, 1064–1079, https://doi.org/10.1093/nar/gkv1021 (2016).
37. Fousteri, M. I. & Lehmann, A. R. A novel SMC protein complex in Schizosaccharomyces pombe contains the Rad18 DNA repair protein. *EMBO J.* **19**, 1691–1702 (2000).
38. Kamada, K., Miyata, M. & Hirano, T. Molecular basis of SMC ATPase activation: role of internal structural changes of the regulatory subcomplex ScpAB. *Structure* **21**, 581–594, https://doi.org/10.1016/j.str.2013.02.016 (2013).
39. Woo, J. S. *et al*. Structural studies of a bacterial condensin complex reveal ATP-dependent disruption of intersubunit interactions. *Cell.* **136**, 85–96 (2009).
40. Gloyd, M., Ghirlando, R. & Guarné, A. The role of MukE in assembling a functional MukBEF complex. *J. Mol. Biol.* **412**, 578–590, https://doi.org/10.1016/j.jmb.2011.08.009 (2011).
41. Pebernard, S., Wohlschlegel, J., McDonald, W. H., Yates, J. R. 3rd & Boddy, M. N. The Nse5-Nse6 dimer mediates DNA repair roles of the Smc5-Smc6 complex. *Mol. Cell Biol.* **26**, 1617–1630 (2006).
42. Ganji, M. *et al*. Real-time imaging of DNA loop extrusion by condensin. *Science*, https://doi.org/10.1126/science.aar7831 (2018).
43. Davidson, I. F. *et al*. DNA loop extrusion by human cohesin. *Science*, https://doi.org/10.1126/science.aaz3418 (2019).
44. Hirano, M. & Hirano, T. Positive and negative regulation of SMC-DNA interactions by ATP and accessory proteins. *Embo J.* **23**, 2664–2673. Epub 2004 Jun 2663. (2004).
45. Ouyang, Z. & Yu, H. Releasing the cohesin ring: A rigid scaffold model for opening the DNA exit gate by Pds5 and Wapl. *Bioessays* **39**, https://doi.org/10.1002/bies.201600207 (2017).
46. Soh, Y. M. *et al*. Molecular basis for SMC rod formation and its dissolution upon DNA binding. *Mol. Cell* **57**, 290–303, https://doi.org/10.1016/j.molcel.2014.11.023 (2015).
47. Chapard, C., Jones, R., van Oepen, T., Scheinost, J. C. & Nasmyth, K. Sister DNA Entrapment between Juxtaposed Smc Heads and Kleisin of the Cohesin Complex. *Mol. Cell* **75**, 224–237.e225, https://doi.org/10.1016/j.molcel.2019.05.023 (2019).
48. Bürmann, F. *et al*. A folded conformation of MukBEF and cohesin. *Nat. Struct. Mol. Biol.* **26**, 227–236, https://doi.org/10.1038/s41594-019-0196-z (2019).
49. Hara, K. *et al*. Structure of cohesin subcomplex pinpoints direct shugoshin-Wapl antagonism in centromeric cohesion. *Nat. Struct. Mol. Biol.* **21**, 864–870, https://doi.org/10.1038/nsmb.2880 (2014).
50. Muir, K. W. *et al*. Structure of the Pds5-Scc1 Complex and Implications for Cohesin Function. *Cell Rep.* **14**, 2116–2126, https://doi.org/10.1016/j.celrep.2016.01.078 (2016).
51. Lee, B. G. *et al*. Crystal Structure of the Cohesin Gatekeeper Pds5 and in Complex with Kleisin Scc1. *Cell Rep.* **14**, 2108–2115, https://doi.org/10.1016/j.celrep.2016.02.020 (2016).
52. Moreno, S., Klar, A. & Nurse, P. Molecular genetic analysis of fission yeast Schizosaccharomyces pombe. *Methods Enzymol.* **194**, 795–823, https://doi.org/10.1016/0076-6879(91)94059-l (1991).
53. Kushnirov, V. V. Rapid and reliable protein extraction from yeast. *Yeast* **16**, 857-860, 10.1002/1097-0061(20000630)16:9<857::aid-yea561>3.0.co;2-b (2000).
54. Zhang, Y. I-TASSER server for protein 3D structure prediction. *BMC Bioinforma.* **9**, 40, https://doi.org/10.1186/1471-2105-9-40 (2008).
55. de Vries, S. J., van Dijk, M. & Bonvin, A. M. The HADDOCK web server for data-driven biomolecular docking. *Nat. Protoc.* **5**, 883–897, https://doi.org/10.1038/nprot.2010.32 (2010).
56. Furmanová, K. *et al*. COZOID: contact zone identifier for visual analysis of protein-protein interactions. *BMC Bioinforma.* **19**, 125, https://doi.org/10.1186/s12859-018-2113-6 (2018).
57. Byska, J., Jurcik, A., Furmanova, K., Kozlikova, B. & Palecek, J. J. Visual Analysis of Protein-Protein Interaction Docking Models Using COZOID Tool. *Methods Mol. Biol.* **2074**, 81–94, https://doi.org/10.1007/978-1-4939-9873-9_7 (2020).

Acknowledgements

We thank C. Hofr for providing the purified His-hTRF2 protein for the ELISA assays. We are grateful to A.R. Lehmann and K. Zabrady for the critical reading of our manuscript. The Czech Science Foundation (GA18-02067S) and the Ministry of Education, Youth and Sports of the Czech Republic project CEITEC 2020 (LQ1601) are acknowledged for funding. AWO is supported by funding from the MRC (Grant Number MR/P018955/1).

Author contributions

J.J.P. and A.W.O. initiated the project. J.J.P. and L.V. designed experiments. L.V., M.A., P.K. and M.N. performed experiments. J.J.P. supervised experiments and wrote the manuscript. All authors reviewed and edited the manuscript.

Competing interests

The authors declare no competing interests.

Additional information

Supplementary information is available for this paper at https://doi.org/10.1038/s41598-020-66647-w.

Correspondence and requests for materials should be addressed to J.J.P.